PROCEEDINGS OF SCIENCE

The spectrum of open confining strings in the large-N_c limit

Alireza Sharifian,[a,*] **Andreas Athenodorou**[b] **and Pedro Bicudo**[a]

[a] *CeFEMA and Physics department, Instituto Superior Técnico, Av. Rovisco Pais, 1049 Lisboa, Portugal*

[b] *Computation-based Science and Technology Research Center, The Cyprus Institute, Cyprus*

E-mail: alireza.sharifian@tecnico.ulisboa.pt, a.athenodorou@cyi.ac.cy, bicudo@tecnico.ulisboa.pt

We compute the spectra of open flux tubes formed between a static quark-antiquark pair for various gauge groups in the large-N_c limit, focusing on different symmetries manifested by the quantum numbers of angular momentum, parity, and charge conjugation. Specifically, we present spectra from $N_c = 3$ up to $N_c = 6$ and for eight different irreducible representations of the symmetry characterizing the flux tube. In this study, we employed an anisotropic Wilson action, a large number of suitable spacial operators, and solved the generalized eigenvalue problem (GEVP) to obtain a significant number of excitations for different combinations of flux tube quantum numbers. The spectra are compared with the Nambu-Goto string model, revealing novel phenomena such as the presence of massive axions in the flux tube spectrum. We find that the mass of the axion in the open flux tube spectra sector is consistent with the mass obtained in the closed flux tube sector.

The 41st International Symposium on Lattice Field Theory (LATTICE2024)
28 July - 3 August 2024
Liverpool, UK

*Speaker

PoS(LATTICE2024)467

1. Preamble

In confining gauge theories such as $SU(N_c)$ gluodynamics, the energy of a gauge field from color charges can be compressed into flux tubes, forming confining strings. Understanding the dynamics of the worldsheet of these strings is crucial for comprehending color confinement. Over the past decade, significant advancements have been made in understanding the effective string theoretical description of the *closed* flux tube [1, 2]. Notably, the dynamics of the worldsheet theory have been derived from lattice data in a model-independent manner. This analysis revealed the presence of several string-like states and a massive excitation known as the worldsheet axion. However, a similar investigation is lacking for the case of the *open* flux tube. In this work, we shed light on the large-N_c limit of the spectrum of open flux-tubes and the existence of axions in their worldsheet.

2. The Nambu-Goto string

A long flux tube can be understood as a low-energy bosonic string. It describes the dynamics of translational $(D-2)$ Goldstone bosons, which exhibit a non-linearly realized $ISO(1,D-1)$ Poincaré symmetry. This symmetry is spontaneously broken to the $ISO(1,1)\times O(D-2)$ subgroup. Consequently, the physics of this string is expected to be described by an action most naturally expressed in terms of D worldsheet scalar fields X^μ, which represent the embedding of the string worldsheet into the target spacetime. The leading term of this action, in terms of the string tension σ, is the simplest bosonic string model, namely the Nambu-Goto action given by:

$$S = -\sigma \int \mathrm{d}^2x \sqrt{-\det h_{\alpha\beta}}\,, \tag{1}$$

where σ is the string tension and $h_{\alpha\beta}$ is the induced metric of the world-sheet, also known as the first fundamental form $h_{\alpha\beta} = \partial_\alpha X^\mu \partial_\beta X_\mu$.

The energy spectrum of an open relativistic string with length R and fixed ends is obtained by quantizing Nambu-Goto is given by:

$$V(R) = \sqrt{\sigma^2 R^2 + 2\pi\sigma\left(N - \frac{(D-2)}{24}\right)}, \tag{2}$$

where N is the quantum number for string vibrations and D is the dimension of space time. This expression is known as the Arvis potential [3].

3. The Axionic String Ansatz (ASA)

In the case of closed flux tubes, the universal predictions of the Thermodynamic Bethe Ansatz (TBA) have been shown to accurately describe a large sector of confining string excitations. This has been confirmed with high precision in both $D = 4$ and $D = 3$ dimensions [4–7]. However, at shorter string lengths R, most states exhibit increasing deviations from these predictions, indicating the influence of non-universal corrections. TBA analysis has allowed for the determination of the first non-trivial Wilson coefficient for $D = 3$ confining strings [8, 9]. Interestingly, some $D = 4$ states show significant deviations from universal TBA predictions even at relatively large R, suggesting

the presence of an additional massive excitation on the string worldsheet, commonly referred to as the "string axion" [1, 8].

This suggests the existence of an additional term in the worldsheet action that governs the leading-order interactions between the worldsheet axion and the transverse Goldstone modes. The corresponding action is given by:

$$S_\phi = \int d^2\sigma\sqrt{-h}\left(-\frac{1}{2}(\partial\phi)^2 - \frac{1}{2}m^2\phi^2 + \frac{Q_\phi}{4}h^{\alpha\beta}\epsilon_{\mu\nu\lambda\rho}\partial_\alpha t^{\mu\nu}\partial_\beta t^{\lambda\rho}\phi\right), \tag{3}$$

where ϕ represents the pseudoscalar worldsheet axion, and $t^{\mu\nu} = \frac{\epsilon^{\alpha\beta}}{\sqrt{-h}}\partial_\alpha X^\mu \partial_\beta X^\nu$. The axion mass m can be determined from Monte Carlo simulations of the 4D $SU(N_c)$ Yang-Mills confining flux tube spectrum using TBA analysis, yielding values of $m = 1.82(2)$ for $SU(3)$, $m = 1.65(2)$ for $SU(5)$ and $m = 1.65(2)$ for $SU(6)$ [10].

4. The quantum numbers of the flux tube

There are three constants of motion whose eigenvalues are used to label the quantum state of the flux tube, illustrated in Fig. 1:

- z-component of angular momentum $\Lambda = 0, 1, 2, 3, \ldots$, they are typically denoted by greek letters Σ, Π, Δ, $\Phi, \ldots$, respectively
- Combination of the charge conjugation and spatial inversion with respect to the mid point of the charge axis operators $\mathcal{P}oC$, its eigenvalues $\eta = 1, -1$, they are denoted by g, u, respectively.
- For $\Sigma(\Lambda = 0)$, reflection with respect to a plan containing the charge axis, $\mathcal{P}_x$, with eigenvalues $\epsilon = +, -$.

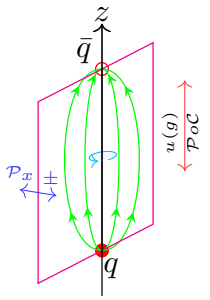

Figure 1: The possible quantum numbers are: Σ_g^+, Σ_g^-, Σ_u^+,Σ_u^-,Π_g,Π_u, Δ_u,Δ_g, ...

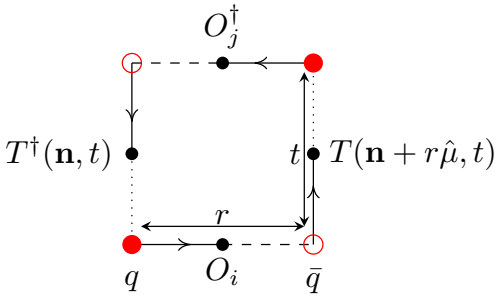

Figure 2: A closed loop corresponds to the entry $C_{i,j}(r, t)$ of the Wilson correlation matrix.

5. Our lattice framework to study the flux tube

In this work, we focus on the large-distance behavior of the excited spectrum, deliberately avoiding short-distance effects. To achieve this, we employ the Wilson action discretized on anisotropic

Ensemble	N_c	β	ξ	ξ_r	Volume	$a_t\sqrt{\sigma}$	$a_s\sqrt{\sigma}$
$W_{3,2}$	3	5.90	2.00	2.1737(4)	$24^3 \times 48$	0.1403(8)	0.3049(17)
$W_{3,4}$	3	5.70	4.00	4.5363(8)	$24^3 \times 96$	0.0887(4)	0.4023(16)
$W_{4,2}$	4	10.70	2.00	2.0958(2)	$24^3 \times 48$	0.1680(2)	0.3521(5)
$W_{4,4}$	4	10.40	4.00	4.2940(5)	$24^3 \times 96$	0.1018(3)	0.4372(12)
$W_{5,2}$	5	17.20	2.00	2.0596(1)	$24^3 \times 48$	0.1451(3)	0.2988(5)
$W_{5,4}$	5	16.50	4.00	4.1853(3)	$24^3 \times 96$	0.1025(0)	0.4288(1)
$W_{6,4}$	6	24.00	4.00	4.1274(2)	$24^3 \times 96$	0.0996(0)	0.4113(2)

Table 1: Details of the ensembles generated using the anisotropic Wilson action. ξ_r is the normalized anisotropy factor, calculated following the instructions in Ref. [12]. Each ensemble comprises 1000 configurations. All ensembles have undergone 100 times multihit smearing in the temporal direction and APE smearing ($\alpha = 0.3$, $n_s = 20$) in the spatial directions.

lattices, which is expressed as:

$$S_{\text{Wilson}} = \beta \left(\frac{1}{\xi} \sum_{x,s>s'} W_{s,s'} + \xi \sum_{x,s} W_{s,t} \right), \tag{4}$$

where $\beta = 6/g^2$ is the inverse coupling constant and ξ represents the bare anisotropy factor, defined as the ratio of the spatial to temporal lattice spacings (a_s/a_t). Furthermore, with s, s' we denote spatial links in different directions. Here, $P_{s,s'}$ represents the spatial plaquettes, and $P_{s,t}$ the spatial-temporal plaquettes. By using an anisotropic action, we achieve finer lattice spacing in the temporal direction while maintaining a coarser spacing in spatial directions. This results in more data points for the effective mass plot and enables the study of larger distances.

In this work, we use the publicly accessible code introduced in Ref. [11] to generate $SU(N_c)$ lattice QCD pure gauge configurations, developed using CUDA to run on GPUs. Parameters of each ensemble are listed in Table 1. We ensure that simulations are ergodic by investigating the topological charge and its evolution.

To compute the spectra of the flux tube, we first calculate the Wilson correlation matrix $C(r,t)$. The entry $C_{i,j}(r,t)$ of the Wilson correlation matrix is the expectation value of spatial-temporal closed loops (Fig. 2), where the spatial sides are replaced with operators O_i and O_j that have identical symmetry to the flux tube of interest.

For example, O_i and O_j can be constructed using the staples shown in Figs. 3 to 6.

Next, we find the generalized eigenvalues λ of the Wilson correlation matrix:

$$C(r,t)\vec{v}_n = \lambda_n(r,t)C(r,t_0)\vec{v}_n, \tag{5}$$

where we set $t_0 = 0$. Consequently, we obtain a set of time-dependent eigenvalues $\lambda_n(t)$ for each r. We then order the eigenvalues and plot the effective mass defined as:

$$E_i(r) = \ln \frac{\lambda_i(r,t)}{\lambda_i(r,t+1)}. \tag{6}$$

The value of the plateau in the effective mass plot corresponds to the energy $E_i(r)$ of the flux tube.

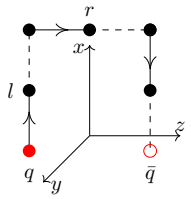

Figure 3: Staples for Σ_g^+, Π_u, and Δ_g flux tubes.

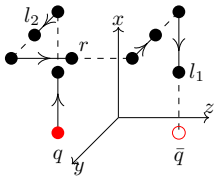

Figure 4: Staples for Σ_g^- flux tubes.

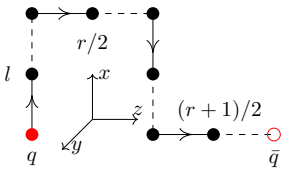

Figure 5: Staples for Σ_u^+,O^{Π_g},and O^{Δ_u} flux tubes.

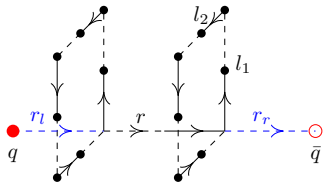

Figure 6: Staples for Σ_u^- flux tubes.

In this work, we use the operators and techniques, already used in Refs. [13, 14] to study $SU(3)$ spectra. Figs. 3 to 6 are the shapes of the stables used to build up the operators for different flux tube symmetries.

6. Results on the spectrum of the open flux-tube

In this section, we present our findings on the spectra for $N_c = 5$ and $N_c = 6$, the largest values of N_c considered in this study, across the eight irreducible representations: Σ_g^+, Σ_g^-, Σ_u^+, Σ_u^-, Π_g, Π_u, Δ_g, and Δ_u. The spectra for these representations are displayed in Figures 7 and 8 for $N_c = 5$ and $N_c = 6$, respectively. For $SU(5)$, we present results at two different lattice spacings to examine whether the spectrum's behavior changes as we approach the continuum limit.

The absolute ground state corresponds to the Σ_g^+ representation, closely approximated by the Arvis potential to a remarkable degree. Deviations of the leading order in $1/(R\sqrt{\sigma})^4$, as derived in [15], are expected. However, the focus of this work is not on subleading corrections in each state's energy but rather on comparing the spectra with the Nambu-Goto string to investigate potential axion signatures. This ground state can be interpreted as the vacuum state $|0\rangle$, with no phonon operators acting on it, implying that no scattering processes occur along the string's worldsheet. Thus, we expect the spectrum to be well-represented by the Nambu-Goto model.

The first higher excited state one can find in the spectrum is ground state of Π_u which is presented in orange colour in the third row from top and second column. This state agrees to a quite good accuracy with the Nambu-Goto state with $N = 1$ meaning that it "carries" only one phonon with one unit of momentum. This is not surprising if one considers again the contributions coming from scattering processes along the world-sheet do not exist. Using the creation/annihilation phonon operators, this state has the form $\alpha_\pm^\dagger|0\rangle$ [16].

As we examine higher excited states, we observe that some begin to show significant deviations from Nambu-Goto behavior, with stricking pattern seen in the ground state of Σ_g^- and across the entire spectrum of states for Σ_u^-. These states exhibit behavior akin to that of a ground state with an additional constant mass term coupled, as illustrated in Figs. 7 and 8. This behavior aligns with

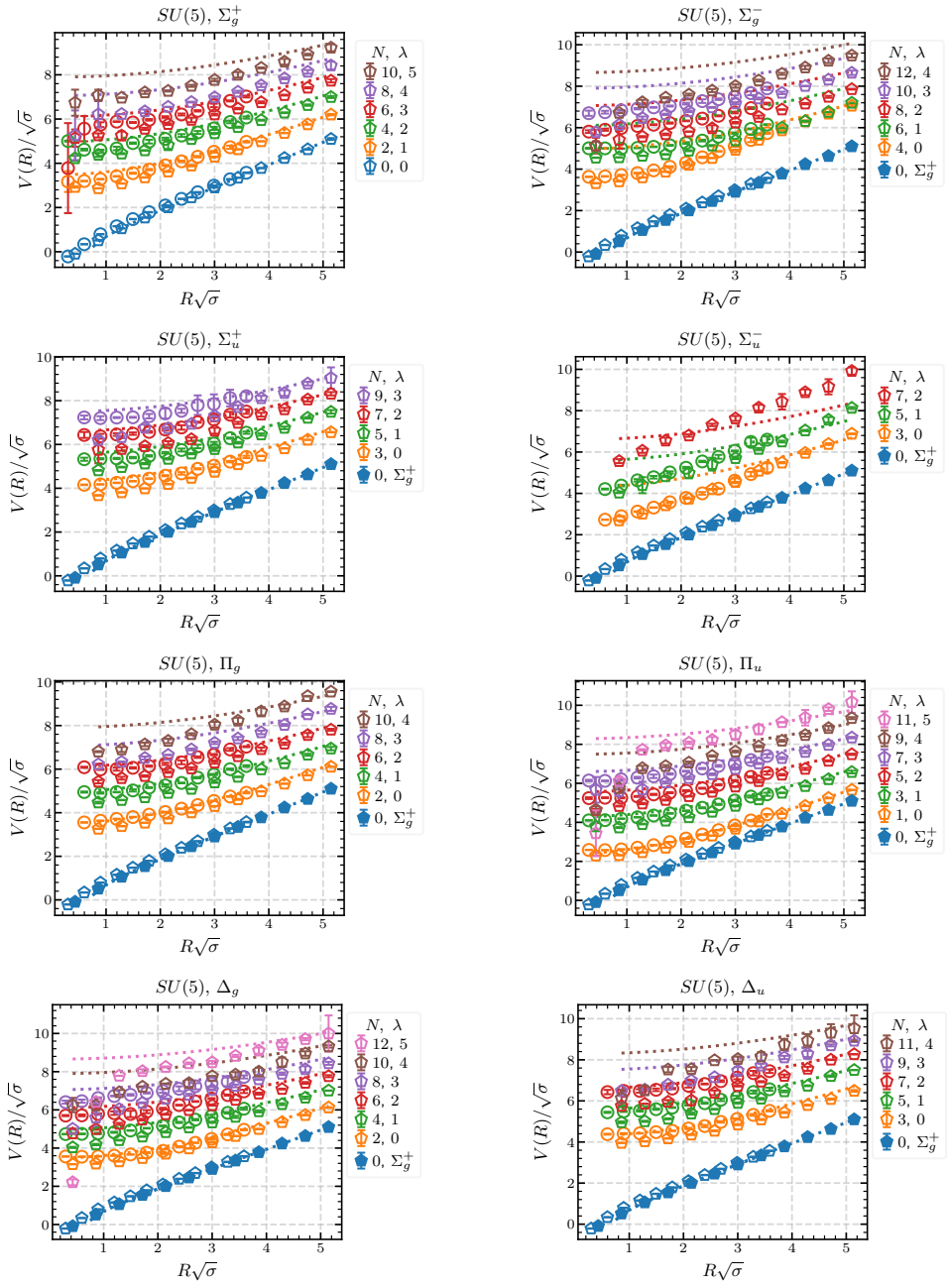

Figure 7: Eight SU(5) spectra. Polygonal shapes in each figure show the simulation with $\xi = 4$, while circle markers indicate $\xi = 2$. N is the quantum number as defined in Eq. 2, and λ is the excitation number.

expectations for an axion coupled to the string. In Fig. 9, we highlight the presence of axion states in these open flux tubes, with the lightest possessing mass same as the axion observed in the closed flux tube spectra.

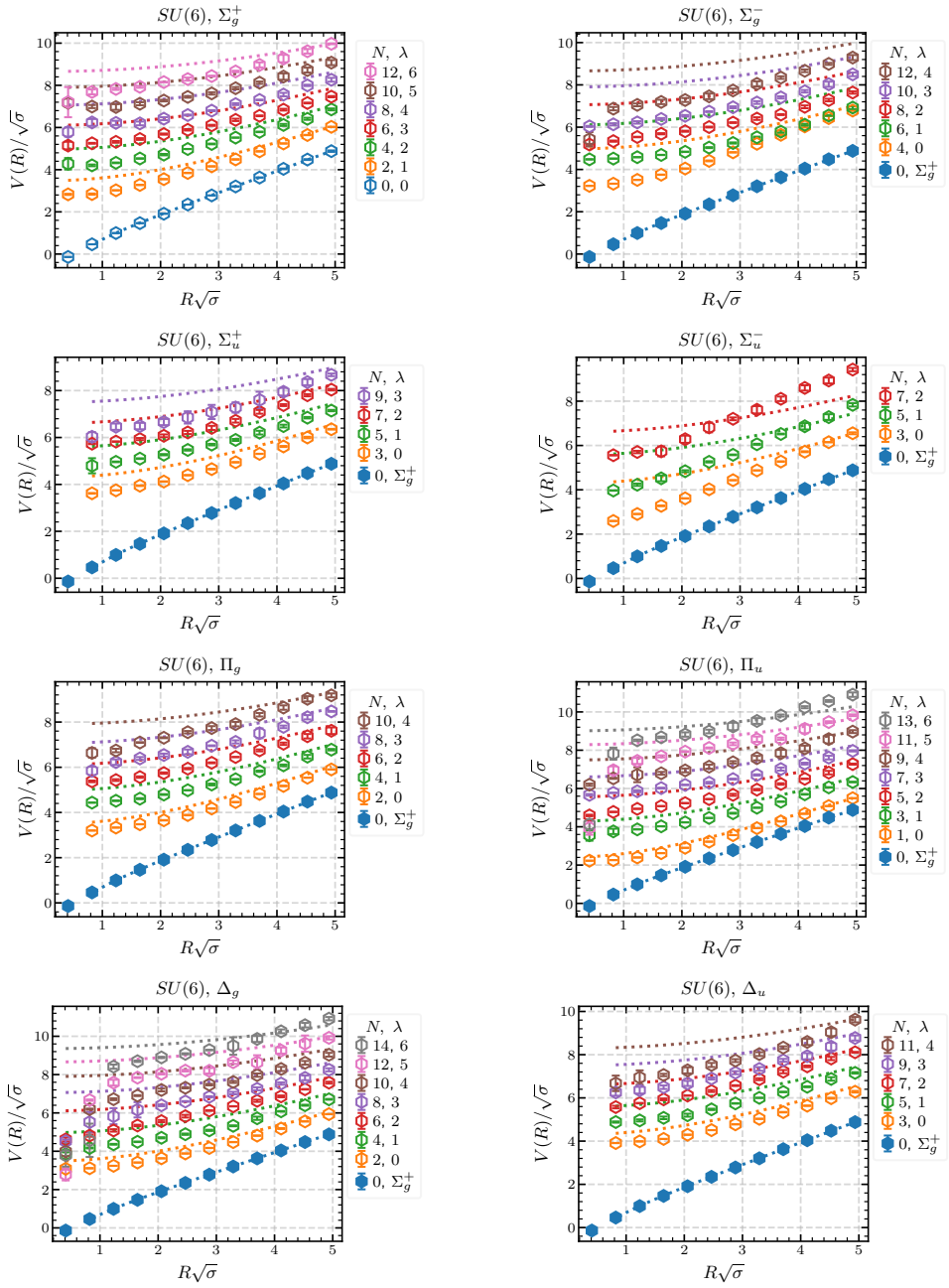

Figure 8: Eight SU(6) spectra. Polygonal shapes in each figure show the simulation with $\xi = 4$, while circle markers indicate $\xi = 2$. N is the quantum number as defined in Eq. 2, and λ is the excitation number.

7. Conclusion

In this study, we conducted a comprehensive analysis of the spectrum of the open flux tube across various discrete symmetry configurations and a large range of excitation levels. Specifically, we extracted the spectrum for $SU(3)$ gauge theories at two lattice spacings, $SU(4)$ and $SU(5)$ each at two lattice spacings, and $SU(6)$ at one lattice spacing. Our results show minimal finite lattice spacing effects and N_c effects, indicating that the observed physics closely represents the large-N_c limit and the continuum.

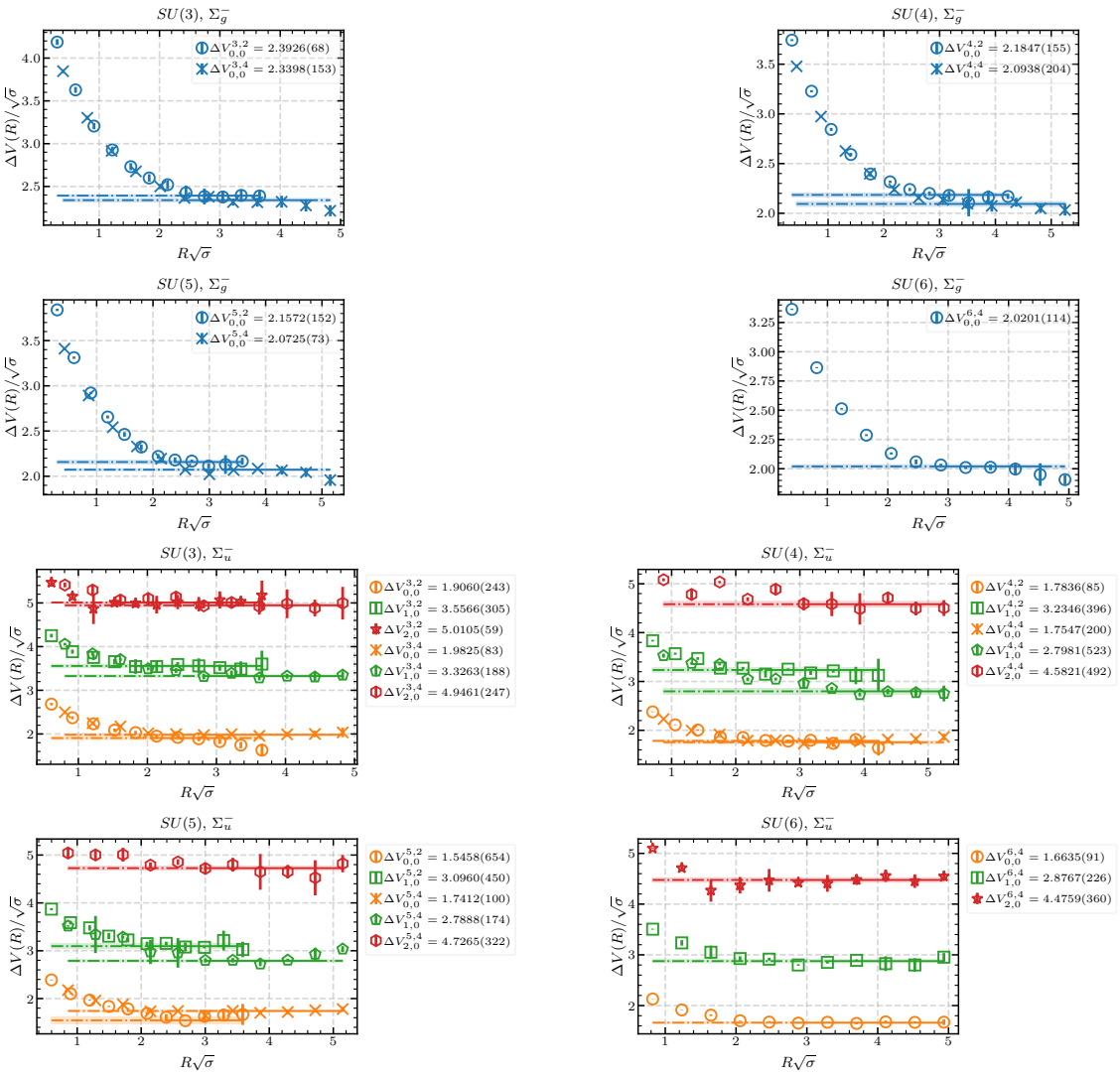

Figure 9: We subtract the groundstate potential to find evidence for axions, for different groups. $\Delta V^{m,n}_{p,0}$ indicates the data from ensemble $W_{m,n}$ in Table 1, and $V_{\Sigma_u^{-}{}^p} - V_{\Sigma_g^+}$ where p is the excitation number.

Our findings reveal that many states in the low-lying spectrum of the flux tube can be well approximated by the Nambu-Goto string model with moderate corrections. However, several states exhibit significant deviations from the Nambu-Goto string behavior, displaying characteristics of massive excitations. Notably, a number of these massive "axionic" excitations were observed, with the lightest having a mass matching its counterpart found in the close flux tube.

Acknowledgments

AS was supported by CEFEMA UIDB/04540/2020 Post-Doctoral Research Fellowship. AA acknowledges support by the "EuroCC" project funded by the "Deputy Ministry of Research, Innovation and Digital Policy and the Cyprus Research and Innovation Foundation" as well as by the EuroHPC JU under grant agreement No 101101903. The authors thank CeFEMA, an IST research unit whose activities are partially funded by FCT contract UIDB/04540/2020 for R&D Units. AA is also indebted to Conghuan Luo for performing a critical review of the manuscript.

References

[1] S. Dubovsky, R. Flauger and V. Gorbenko, *Evidence from Lattice Data for a New Particle on the Worldsheet of the QCD Flux Tube*, *Phys. Rev. Lett.* **111** (2013) 062006 [1301.2325].

[2] A. Athenodorou and M. Teper, *The torelon spectrum and the world-sheet axion*, *PoS* **LATTICE2021** (2022) 103 [2112.11213].

[3] J. Arvis, *The exact $q\bar{q}$ potential in nambu string theory*, *Phys. Lett. B* **127** (1983) 106.

[4] A. Athenodorou, B. Bringoltz and M. Teper, *Closed flux tubes and their string description in D=3+1 SU(N) gauge theories*, *JHEP* **02** (2011) 030 [1007.4720].

[5] A. Athenodorou, B. Bringoltz and M. Teper, *Closed flux tubes and their string description in D=2+1 SU(N) gauge theories*, *JHEP* **05** (2011) 042 [1103.5854].

[6] A. Athenodorou and M. Teper, *On the spectrum and string tension of U(1) lattice gauge theory in 2 + 1 dimensions*, *JHEP* **01** (2019) 063 [1811.06280].

[7] A. Athenodorou, S. Dubovsky, C. Luo and M. Teper, *Excitations of Ising strings on a lattice*, *JHEP* **05** (2023) 082 [2301.00034].

[8] S. Dubovsky, R. Flauger and V. Gorbenko, *Flux Tube Spectra from Approximate Integrability at Low Energies*, *J. Exp. Theor. Phys.* **120** (2015) 399 [1404.0037].

[9] C. Chen, P. Conkey, S. Dubovsky and G. Hernández-Chifflet, *Undressing Confining Flux Tubes with $T\bar{T}$*, *Phys. Rev. D* **98** (2018) 114024 [1808.01339].

[10] A. Athenodorou, S. Dubovsky, C. Luo and M. Teper, *Confining Strings and the Worldsheet Axion from the Lattice*, 2411.03435.

[11] N. Cardoso and P. Bicudo, *Generating $SU(N_c)$ pure gauge lattice QCD configurations on GPUs with CUDA and OpenMP*, *Comput. Phys. Commun.* **184** (2013) 509 [1112.4533].

[12] I.T. Drummond, A. Hart, R.R. Horgan and L.C. Storoni, *One loop calculation of the renormalized anisotropy for improved anisotropic gluon actions on a lattice*, *Phys. Rev. D* **66** (2002) 094509 [hep-lat/0208010].

[13] A. Sharifian, N. Cardoso and P. Bicudo, *Eight very excited flux tube spectra and possible axions in SU(3) lattice gauge theory*, *Phys. Rev. D* **107** (2023) [2303.15152].

[14] P. Bicudo, N. Cardoso and A. Sharifian, *Spectrum of very excited Σ_g^+ flux tubes in SU(3) gauge theory*, *Phys. Rev. D* **104** (2021) 054512 [2105.12159].

[15] O. Aharony and E. Karzbrun, *On the effective action of confining strings*, *JHEP* **06** (2009) 012 [0903.1927].

[16] K.J. Juge, J. Kuti and C. Morningstar, *Excitations of the static quark anti-quark system in several gauge theories*, in *Proceedings of Wako 2003, Color Confinement and Hadrons in Quantum Chromodynamics* (2004), 221 [hep-lat/0312019].